



# High accuracy, high resolution $^{235}\text{U}(n,f)$ cross section from n\_TOF (CERN) from 18 meV to 10 keV

M. Mastromarco<sup>1,2</sup>, S. Amaducci<sup>3,a</sup> , N. Colonna<sup>1</sup>, P. Finocchiaro<sup>3</sup>, L. Cosentino<sup>3</sup>, M. Barbagallo<sup>7</sup>, O. Aberle<sup>7</sup>, J. Andrzejewski<sup>8</sup>, L. Audouin<sup>9</sup>, M. Bacak<sup>10,7,11</sup>, J. Balibrea<sup>12</sup>, F. Bečvář<sup>13</sup>, E. Berthoumieux<sup>11</sup>, J. Billowes<sup>14</sup>, D. Bosnar<sup>15</sup>, A. Brown<sup>16</sup>, M. Caamaño<sup>17</sup>, F. Calviño<sup>18</sup>, M. Calviani<sup>7</sup>, D. Cano-Ott<sup>12</sup>, R. Cardella<sup>7</sup>, A. Casanovas<sup>18</sup>, F. Cerutti<sup>7</sup>, Y. H. Chen<sup>9</sup>, E. Chiaveri<sup>7,14,19</sup>, G. Cortés<sup>18</sup>, M. A. Cortés-Giraldo<sup>19</sup>, L. A. Damone<sup>3,20</sup>, M. Diakaki<sup>11</sup>, C. Domingo-Pardo<sup>21</sup>, D. Diacono<sup>1</sup>, R. Dressler<sup>22</sup>, E. Dupont<sup>11</sup>, I. Durán<sup>17</sup>, B. Fernández-Domínguez<sup>17</sup>, A. Ferrari<sup>7</sup>, P. Ferreira<sup>23</sup>, V. Furman<sup>24</sup>, K. Göbel<sup>25</sup>, A. R. García<sup>12</sup>, A. Gawlik<sup>8</sup>, S. Gilardoni<sup>7</sup>, T. Glodariu<sup>26</sup>, I. F. Gonçalves<sup>23</sup>, E. González-Romero<sup>12</sup>, E. Griesmayer<sup>10</sup>, C. Guerrero<sup>19</sup>, F. Gunsing<sup>11,7</sup>, H. Harada<sup>27</sup>, S. Heinitz<sup>22</sup>, J. Heyse<sup>28</sup>, D. G. Jenkins<sup>16</sup>, E. Jericha<sup>10</sup>, F. Käppeler<sup>29</sup>, Y. Kadi<sup>7</sup>, A. Kalamara<sup>30</sup>, P. Kavrigin<sup>10</sup>, A. Kimura<sup>27</sup>, N. Kivel<sup>22</sup>, I. Knapova<sup>13</sup>, M. Kokkoris<sup>30</sup>, M. Krťička<sup>13</sup>, D. Kurtulgu<sup>25</sup>, E. Leal-Cidoncha<sup>17</sup>, C. Lederer<sup>31</sup>, H. Leeb<sup>10</sup>, J. Leredegui-Marco<sup>19</sup>, S. Lo Meo<sup>4,5</sup>, S. J. Lonsdale<sup>31</sup>, D. Macina<sup>7</sup>, A. Manna<sup>5,6</sup>, J. Marganec<sup>8,32</sup>, T. Martínez<sup>12</sup>, A. Masi<sup>7</sup>, C. Massimi<sup>5,6</sup>, P. Mastinu<sup>33</sup>, E. A. Maugeri<sup>22</sup>, A. Mazzone<sup>3,34</sup>, E. Mendoza<sup>12</sup>, A. Mengoni<sup>4,5</sup>, P. M. Milazzo<sup>35</sup>, F. Mingrone<sup>7</sup>, A. Musumarra<sup>3,36</sup>, A. Negret<sup>26</sup>, R. Nolte<sup>32</sup>, A. Oprea<sup>26</sup>, N. Patronis<sup>37</sup>, A. Pavlik<sup>38</sup>, J. Perkowski<sup>8</sup>, I. Porras<sup>39</sup>, J. Praena<sup>39</sup>, J. M. Quesada<sup>19</sup>, D. Radeck<sup>32</sup>, T. Rauscher<sup>40,41</sup>, R. Reifarth<sup>25</sup>, C. Rubbia<sup>7</sup>, J. A. Ryan<sup>14</sup>, M. Sabaté-Gilarte<sup>7,19</sup>, A. Saxena<sup>42</sup>, P. Schillebeeckx<sup>28</sup>, D. Schumann<sup>22</sup>, P. Sedyshev<sup>24</sup>, A. G. Smith<sup>14</sup>, N. V. Sosnin<sup>14</sup>, A. Stamatopoulos<sup>30</sup>, G. Tagliente<sup>3</sup>, J. L. Tain<sup>21</sup>, A. Tarifeño-Saldivia<sup>18</sup>, L. Tassan-Got<sup>9</sup>, S. Valenta<sup>13</sup>, G. Vannini<sup>5,6</sup>, V. Variale<sup>3</sup>, P. Vaz<sup>23</sup>, A. Ventura<sup>5</sup>, V. Vlachoudis<sup>7</sup>, R. Vlastou<sup>30</sup>, A. Wallner<sup>43</sup>, S. Warren<sup>14</sup>, C. Weiss<sup>10</sup>, P. J. Woods<sup>31</sup>, T. Wright<sup>14</sup>, P. Žugec<sup>15,7</sup>

- <sup>1</sup> Istituto Nazionale di Fisica Nucleare, Sezione di Bari, Italy  
<sup>2</sup> Dipartimento Interateneo di Fisica, Università degli Studi di Bari, Bari, Italy  
<sup>3</sup> INFN Laboratori Nazionali del Sud, Catania, Italy  
<sup>4</sup> Agenzia Nazionale per le Nuove Tecnologie (ENEA), Bologna, Italy  
<sup>5</sup> Istituto Nazionale di Fisica Nucleare, Sezione di Bologna, Bologna, Italy  
<sup>6</sup> Dipartimento di Fisica e Astronomia, Università di Bologna, Bologna, Italy  
<sup>7</sup> European Organization for Nuclear Research (CERN), Meyrin, Switzerland  
<sup>8</sup> University of Lodz, Genève, Poland  
<sup>9</sup> Institut de Physique Nucléaire, CNRS-IN2P3, University Paris-Sud, Université Paris-Saclay, 91406 Orsay Cedex, France  
<sup>10</sup> Technische Universität Wien, Vienna, Austria  
<sup>11</sup> CEA Irfu, Université Paris-Saclay, 91191 Gif-sur-Yvette, France  
<sup>12</sup> Centro de Investigaciones Energéticas Medioambientales y Tecnológicas (CIEMAT), Madrid, Spain  
<sup>13</sup> Charles University, Prague, Czech Republic  
<sup>14</sup> University of Manchester, Manchester, UK  
<sup>15</sup> Department of Physics, Faculty of Science, University of Zagreb, Zagreb, Croatia  
<sup>16</sup> University of York, Heslington, UK  
<sup>17</sup> University of Santiago de Compostela, Santiago, Spain  
<sup>18</sup> Universitat Politècnica de Catalunya, Barcelona, Spain  
<sup>19</sup> Universidad de Sevilla, Seville, Spain  
<sup>20</sup> Dipartimento di Fisica, Università degli Studi di Bari, Bari, Italy  
<sup>21</sup> Instituto de Física Corpuscular, CSIC-Universidad de Valencia, Valencia, Spain  
<sup>22</sup> Paul Scherrer Institut (PSI), Villigen, Switzerland  
<sup>23</sup> Instituto Superior Técnico, Lisbon, Portugal  
<sup>24</sup> Joint Institute for Nuclear Research (JINR), Dubna, Russia  
<sup>25</sup> Goethe University, Frankfurt, Germany  
<sup>26</sup> Horia Hulubei National Institute of Physics and Nuclear Engineering, Bucharest, Romania  
<sup>27</sup> Japan Atomic Energy Agency (JAEA), Tokai-mura, Japan  
<sup>28</sup> European Commission, Joint Research Centre (JRC), Geel, Belgium  
<sup>29</sup> Karlsruhe Institute of Technology, Campus North, IKP, 76021 Karlsruhe, Germany  
<sup>30</sup> National Technical University of Athens, Athens, Greece  
<sup>31</sup> School of Physics and Astronomy, University of Edinburgh, Edinburgh, UK  
<sup>32</sup> Physikalisch-Technische Bundesanstalt (PTB), Bundesallee 100, 38116 Brunswick, Germany  
<sup>33</sup> Istituto Nazionale di Fisica Nucleare, Sezione di Legnano, Legnano, Italy  
<sup>34</sup> Consiglio Nazionale Delle Ricerche, Bari, Italy

- <sup>35</sup> Istituto Nazionale di Fisica Nucleare, Sezione di Trieste, Trieste, Italy  
<sup>36</sup> Dipartimento di Fisica e Astronomia, Università di Catania, Catania, Italy  
<sup>37</sup> University of Ioannina, Ioannina, Greece  
<sup>38</sup> Faculty of Physics, University of Vienna, Vienna, Austria  
<sup>39</sup> University of Granada, Granada, Spain  
<sup>40</sup> Department of Physics, University of Basel, Basel, Switzerland  
<sup>41</sup> Centre for Astrophysics Research, University of Hertfordshire, Hertfordshire, UK  
<sup>42</sup> Bhabha Atomic Research Centre (BARC), Trombay, India  
<sup>43</sup> Australian National University, Mumbai, Australia

Received: 1 March 2022 / Accepted: 30 June 2022

© The Author(s) 2022

Communicated by Navin Alahari.

**Abstract** The  $^{235}\text{U}(n,f)$  cross section was measured in a wide energy range (18 meV–170 keV) at the n\_TOF facility at CERN, relative to  $^6\text{Li}(n,t)$  and  $^{10}\text{B}(n,\alpha)$  standard reactions, with high resolution and accuracy, with a setup based on a stack of six samples and six silicon detectors placed in the neutron beam. In this paper we report on the results in the region between 18 meV and 10 keV neutron energy. A resonance analysis has been performed up to 200 eV, with the code SAMMY. The resulting fission kernels are compared with the ones extracted on the basis of the resonance parameters of the most recent major evaluated data libraries. A comparison of the n\_TOF data with the evaluated cross sections is also performed from thermal to 10 keV neutron energy for the energy-averaged cross section in energy groups of suitably chosen width. A good agreement, within 0.5%, is found on average between the new results and the latest evaluated data files ENDF/B-VIII.0 and JEFF-3.3, as well as with respect to the broad group average fission cross section established in the framework of the standard working group of IAEA (the so-called reference file). However, some discrepancies, of up to 4%, are still present in some specific energy regions. The new dataset here presented, characterized by a unique combination of high resolution and accuracy, low background and wide energy range, can help to improve the evaluations from the Resolved Resonance Region up to 10 keV, also reducing the uncertainties that affect this region.

## 1 Introduction

The neutron-induced fission of  $^{235}\text{U}$  is one of the most important reactions for applications, in particular related to energy production. Its cross section at thermal and from 0.15 to 200 MeV neutron energy is an established standard, widely employed in a variety of fields, from neutron flux measurements to dose evaluation for radiation protection purposes [1]. Outside the standard range, the  $^{235}\text{U}(n,f)$  cross section can also be used as reference, although the presence of

resonances and resonance-like structures up to  $\sim 10$  keV makes the use of this cross section less straightforward. While recently the cross section integral between 7.8 and 11 eV has been adopted as an additional standard, with associated uncertainty of 1.2%, uncertainties of the order of a few percent still persist in the Resolved Resonance Region (RRR, corresponding to  $E_n < 2.25$  keV), as well in the Unresolved Resonance Region (URR, extending up to 25 keV), with some discrepancies between different evaluated data files.

In order to try to solve discrepancies in current libraries for  $^{235}\text{U}$  and other key isotopes relevant for nuclear applications, a Collaborative International Evaluation Library Organization (CIELO) was established in 2013, coordinated by the Nuclear Energy Agency (NEA) of the Organization for Economic Cooperation and Development (OECD). A detailed description of this project and related results can be found in [2]. Despite the achieved progress within this framework for several reactions, open questions and differences in the evaluations still remain, documented in two different datasets, adopted by different evaluated data libraries. Differences of the order of a few percent still persist on some crucial reactions, including the  $^{235}\text{U}(n,f)$  reaction outside the standard region. In an attempt to reduce the uncertainties, new collaborative efforts are being undertaken, such as the INDEN project coordinated by IAEA [3], that aims at improving the evaluation methodology and producing updated nuclear data files. In this respect, while re-analysis and combination of previous data can lead to some improvements, a major uncertainty reduction can be achieved by incorporating new, high resolution and high accuracy data, that can help to sort out existing discrepancies. In this respect, the n\_TOF facility [4] is currently one of the best suited facilities worldwide for collecting new data on the  $^{235}\text{U}(n,f)$  cross sections in the Resolved and Unresolved Resonance Regions, thanks to the very convenient features of the neutron beam, in particular the high resolution, the wide energy range and the low background. An overview of the facility and of the fission experimental program at n\_TOF can be found in [5].

Data from n\_TOF in the RRR collected with Parallel Plate Avalanche Counters (PPAC) (Ref. [6], hereafter referred to as Paradela's data) were already made available in 2016, and have been used in the recent ENDF/B-VIII and JEFF-3.3

T. Glodariu, F. Käppler: Deceased.

<sup>a</sup> e-mail: amaducci@lns.infn.it (corresponding author)

evaluations. On average they showed a good agreement up to 2 keV with the IAEA reference file (being  $\sim 1\%$  lower), while a larger difference was observed relative to ENDF/B-VII (being  $\sim 2\%$  higher). A difference of 3% has also been reported by Capote et al. [7] between ENDF/B-VII and the new IAEA CIELO evaluated cross section between 100 eV and 2.25 keV (the latter being consistent with the IAEA 2017 reference file, see Fig. 2 in [7]). We recall that the ENDF/B-VIII.0 evaluation, officially released in 2018 [8, 9], has now adopted the IAEA CIELO evaluations for the considered reaction. Paradela's data in the RRR [6, 10] have also been used in the new JEFF-3.3 evaluation, officially released in 2017 [11] 12. However, as will be shown in this work, small differences between ENDF/B-VIII.0 and JEFF-3.3 on the  $^{235}\text{U}(n,f)$  cross section up to 10 keV still persist.

Paradela's data mentioned above were collected in the long flight-base experimental area (EAR1) of n\_TOF, and are therefore characterized by a high resolution ( $\Delta E/E < 10^{-3}$ ). However, those data were not the result of a dedicated measurement relative to a standard, such as the  $^6\text{Li}(n,t)$  or  $^{10}\text{B}(n,\alpha)$ , being the  $^{235}\text{U}$  sample used as reference for other actinide samples measured simultaneously. Rather, the cross section was extracted relative to the neutron flux that had previously been determined on the basis of various standards, including the  $^{235}\text{U}(n,f)$  reaction itself, with a relatively low resolution and an uncertainty of up to 5% in the keV region [13]. Furthermore, the energy range did not extend down to thermal energy, hindering an accurate normalization to a well established standard. As a consequence, the data were normalized to the cross section integral in the region between 7.8 and 11.0 eV, and the value of 246.4 b-eV in the IAEA 2009 reference file was used to that purpose (at that time not yet adopted as an additional standard, the currently adopted standard value being 247.5 b-eV).

Recently, a measurement was performed at n\_TOF specifically dedicated to the high-resolution, high-accuracy measurement of the  $^{235}\text{U}(n,f)$  reaction in the whole energy region from thermal to 170 keV neutron energy. The main aim of that measurement was to investigate a discrepancy that had previously been noted in the 10–30 keV energy range. Details on the measurement, the experimental setup and the analysis procedure can be found in Ref. [14]. The main features of this new dataset are that the  $^{235}\text{U}(n,f)$  cross section is measured directly relative to the  $^6\text{Li}$  and  $^{10}\text{B}$  standards, and that the energy range encompasses the thermal point and extends up to 170 keV, i.e. in the standard regions, so that a high confidence on the absolute normalization can be achieved. The present paper complements the previous publication [14], by reporting the pointwise data in the range from thermal to 10 keV, in an attempt to provide some of the most accurate and high-resolution data achieved so far on the  $^{235}\text{U}(n,f)$  cross section in the Resolved and Unresolved Resonance Region.

The results here reported could help to solve existing discrepancies between different evaluations, providing an important contribution to future upgrades of evaluated libraries and/or ongoing collaborative efforts, such as the INDEN project of IAEA, with the final goal of improving the accuracy of this important cross section in this energy region.

The paper is organized as follows: the main features of the experimental setup and procedure are described in Sect. 2, and cross section determination in Sect. 3. A resonance analysis up to 200 eV is reported in Sect. 4, together with a comparison of the resulting fission kernels with current versions of major libraries. Energy-averaged cross section data from thermal to 10 keV neutron energy are presented and discussed in Sect. 5, in comparison with current and past evaluations and previous experimental data. Conclusions are drawn in Sect. 6.

## 2 Experimental setup and data analysis

The experimental apparatus consists of a stack of six Si-detectors with six samples, two of each  $^6\text{Li}$ ,  $^{10}\text{B}$  and  $^{235}\text{U}$  isotope, mounted in between in a closely-packed geometry [14]. The main features of the setup were: a large solid angle coverage, the possibility of detecting reaction products both in the forward and backward direction, a feature particularly important for the  $^6\text{Li}(n,t)$  and  $^{10}\text{B}(n,\alpha)$  reactions, affected by angular anisotropy of the emitted charged particle that starts becoming relevant for neutron energy above a few keV. Finally, the setup was characterized by a good particle identification capability, of importance for background rejection. The setup was hosted in a vacuum chamber placed on the neutron beam line, with thin windows at the air–vacuum interface. The measurement was performed in the experimental area (EAR1) positioned at the end of the 183.49 (2) m long neutron flight path. In this area, the energy resolution of the neutron beam goes from  $3 \cdot 10^{-4}$  at thermal up to  $10^{-3}$  at 10 keV [4].

The  $^{235}\text{U}(n,f)$  cross section was determined directly relative to the  $^6\text{Li}(n,t)$  and  $^{10}\text{B}(n,\alpha)$  reactions, whose cross sections are standards of measurement all the way from thermal to 1 MeV. Another important feature of the measurement was the large energy range covered, extending from thermal neutron energy to 170 keV. Relative to Paradela's data mentioned above, the new measurement has the advantage of including both the thermal point and an energy region above 150 keV, where the  $^{235}\text{U}(n,f)$  cross section is standard, thus allowing for an accurate normalization of the data in the whole energy range measured. In fact, the dataset here presented is one of the most complete in terms of energy range covered, and accurate in terms of reference reactions used, as well as in normalization. Combined with the high resolution and low background of the n\_TOF neutron beam in EAR1,

the wide energy range and high accuracy makes the present dataset rather unique in the landscape of experimental cross sections available on the  $^{235}\text{U}(n,f)$  reaction in the Resolved and Unresolved Resonance Regions, and suitable for verifying current major evaluations, possibly identifying residual problems (if any). To this aim, we perform here a thorough comparison of the data with three libraries: ENDF/B-VII, ENDF/B-VIII.0 and JEFF-3.3 (evaluated cross sections in the JENDL-5 library are similar to ENDF/B-VIII.0 and are therefore not included in this comparison).

### 3 Cross section determination

The yield with coarse energy binning from thermal to 170 keV neutron energy has already been reported in Ref. [14] and uploaded on the nuclear data repository EXFOR [15]. In this paper we report on the analysis of the data, up to 10 keV, with the higher resolution required to perform a resonance analysis and a more detailed comparison with evaluated data libraries. These data will then be made available on EXFOR for dissemination and possible use in future evaluations of the  $^{235}\text{U}(n,f)$  reaction in the Resolved and Unresolved Resonance Regions.

The main features of the present data, in terms of background, normalization and uncertainty estimates, have mostly been discussed in [14]. We recall here that, thanks to the characteristics of the n\_TOF facility and the low mass of the detectors, the measurement is affected by a negligible background. This feature is particularly important in the valleys between resonances, as it leads on the one hand to a more reliable resonance analysis in the tails, and on the other hand to a more accurate determination of the energy-averaged cross section, both affected by a non-negligible contribution of the valleys. The low background of the measurement is evident in Fig. 1, where the n\_TOF data in the valleys are comparable to, or lower than, the evaluated cross sections, showing in some regions structures not present in the evaluations, and that could have been previously masked by a higher background. These structures are statistically significant, as they cannot be due to contaminants whose content in the samples was certified below  $10^{-6}$ , and in several cases were also observed in Paradela's data [6].

As already mentioned, an important feature of the present data is that the cross section is extracted directly from the ratio of the measured count-rate for the  $^{235}\text{U}$  sample to the reference  $^6\text{Li}$  and  $^{10}\text{B}$  samples. This procedure completely removes the effect of structures, in particular absorption dips, that are typically present in the neutron flux, related to the neutron source itself or to windows at the air-vacuum interface on the neutron beam line. At n\_TOF, the presence of a thick Al window produces several larger dips, while a 0.2% Zn content produces smaller dips that however could lead to

a few percent error in the cross section determination (as will be shown in Sect. 5).

As discussed in [14], the normalization of the measured cross section was performed relative to the cross section integral in the neutron energy range between 7.8 and 11.0 eV, recently adopted as a standard ( $247.5 \pm 3$  b·eV) [16]. The combination of the systematic uncertainty on the standard (1.2%) with the statistical error on the measured integral (0.4%) results in an overall uncertainty of 1.3% up to 1 keV. Above this energy an additional 0.8% uncertainty on the efficiency corrections has to be considered, leading to a total value of 1.5% (being other energy-dependent uncertainties negligible in the range considered in this work). The peculiar features of the n\_TOF neutron beam and of the experimental setup and the adopted procedure for the normalization of the results makes the present measurement one of the most accurate ever performed on this reaction. Finally, a fundamental feature of the present dataset (as compared to most previous ones), is the wide energy range covered in a single measurement, that makes possible to directly compare the data with the  $^{235}\text{U}(n,f)$  cross section standard in two regions, i.e. at thermal and around 150 keV. The very good agreement observed at those energies (shown in Sect. 5) provides high confidence on the cross section values in the whole energy region, here reported.

In the following, we present the results and a comparison with evaluated nuclear data of major libraries, by performing on the one hand a resonance analysis at lower energy, and on the other hand by averaging the measured cross section in wider energy bins up to 10 keV. The present data are also compared with some previous datasets characterized by similar resolution. The new, high accuracy and high resolution data on this important reaction could be beneficial for checking the reliability of current evaluations in major data libraries, possibly identifying residual shortcomings for future updates.

### 4 Resonance analysis

A resonance analysis was performed with the SAMMY code [17], within the Reich–Moore approximation, from thermal to 200 eV. Although the limit of the Resolved Resonance Region is currently assumed at 2.25 keV, and resonance structures are observed even above this limit, in the present work we have considered only resonances up to 200 eV, since at higher energy the clustering of resonances becomes dominant, and the number of missing levels increases. Furthermore, up to this energy the n\_TOF neutron beam resolution function has a negligible influence, being the resolution essentially dominated by Doppler broadening. It should be considered that even at this low energy, several resonance structures are made of clusters of unresolved resonances, due to the small average level spacing, as compared to their

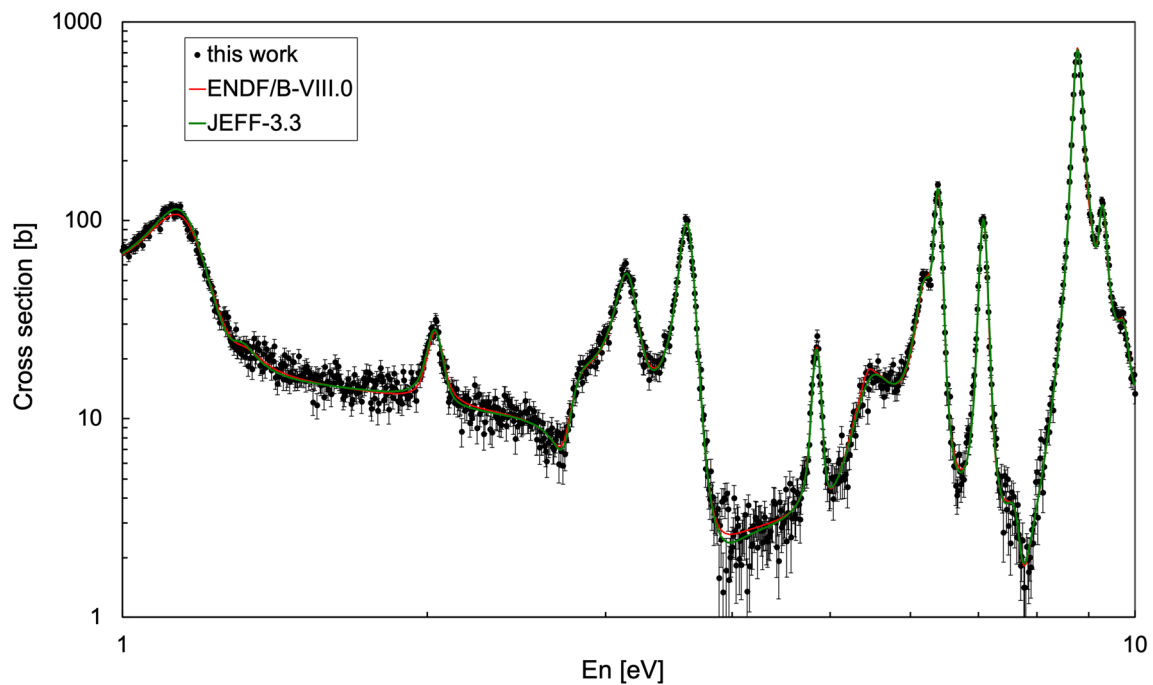


**Fig. 1** Measured  $^{235}\text{U}(n,f)$  cross section in the 1–10 eV neutron energy range, compared with evaluated data. The high resolution of the n\_TOF data makes possible to distinctly observe small structures in the valleys between resonances, clearly testifying the low background

natural width and to the effect of the Doppler broadening. Finally, above 200 eV a more statistically meaningful comparison with libraries and previous datasets can be performed by averaging the cross section in suitably wide energy bins as discussed in Sect. 5.

In the SAMMY fits, initial input parameters of the resonances were taken from the latest evaluated data files, either ENDF/B-VIII.0 or JEFF-3.3. The energy, neutron and capture widths were kept fixed, while both fission widths were left free, with a fudge factor set at 0.1 (corresponding to the possibility of modifying the value by 10% for each iteration). The numerical n\_TOF resolution function was used in the fits. In order to check the consistency of the normalization value for the n\_TOF yields, the corresponding parameter was initially left free when fitting the energy region from 20 meV to 10 eV. The values obtained using initial resonance parameters from the ENDF/B-VIII.0 and JEFF-3.3 were 0.993 and 0.997, respectively, indicating that the normalization of the n\_TOF yield was consistent with evaluated cross sections within a few per mill. For the fits from 10 to 200 eV neutron energy, the normalization parameters were kept fixed at the values mentioned above. For the resonance fits in the whole neutron energy region analysed, the level of background was initially left free, showing that the resulting values were in all cases negligible. Figure 2 shows the experimental data with the results of the SAMMY fit (initial resonance parameters from ENDF/B-VIII.0) in the whole range from thermal to 200 eV neutron energy, along with the residuals defined as

the difference between fit and data divided respectively by the data (and expressed in percent) and by the data standard deviation. The quality of the fits in selected energy regions can also be appreciated in Fig. 3. The experimental fission yield and the result of the resonance analysis performed within this work are represented by the symbols, with their statistical uncertainty, and by the red curve, respectively. They are compared with the fission yield calculated by SAMMY on the basis of the resonance parameters of the two most recent evaluated data libraries, represented in the figures by the green curve (for clarity, the comparison with ENDF/B-VIII.0 and JEFF-3.3 is shown separately). For most resonances, the new fit and evaluated fission yields are indistinguishable, indicating a very good agreement between the n\_TOF data reported here and the evaluated cross sections. In some cases, however, the evaluations fall short of reproducing the observed resonances, as can be inferred from the differences between the red and the green curve in Fig. 3. Most of the differences are observed in the neutron energy range between 20 to 100 eV (as confirmed by the analysis of the energy-averaged cross section in Sect. 5). The ranges in Fig. 3 correspond to regions where larger differences between data and evaluations were found.

A more quantitative comparison can be performed by considering the fission widths. However, although this is clearly the most important parameter to be determined from the resonance analysis of fission data, the values of such width are correlated to the neutron and, to a lesser extent, the capture

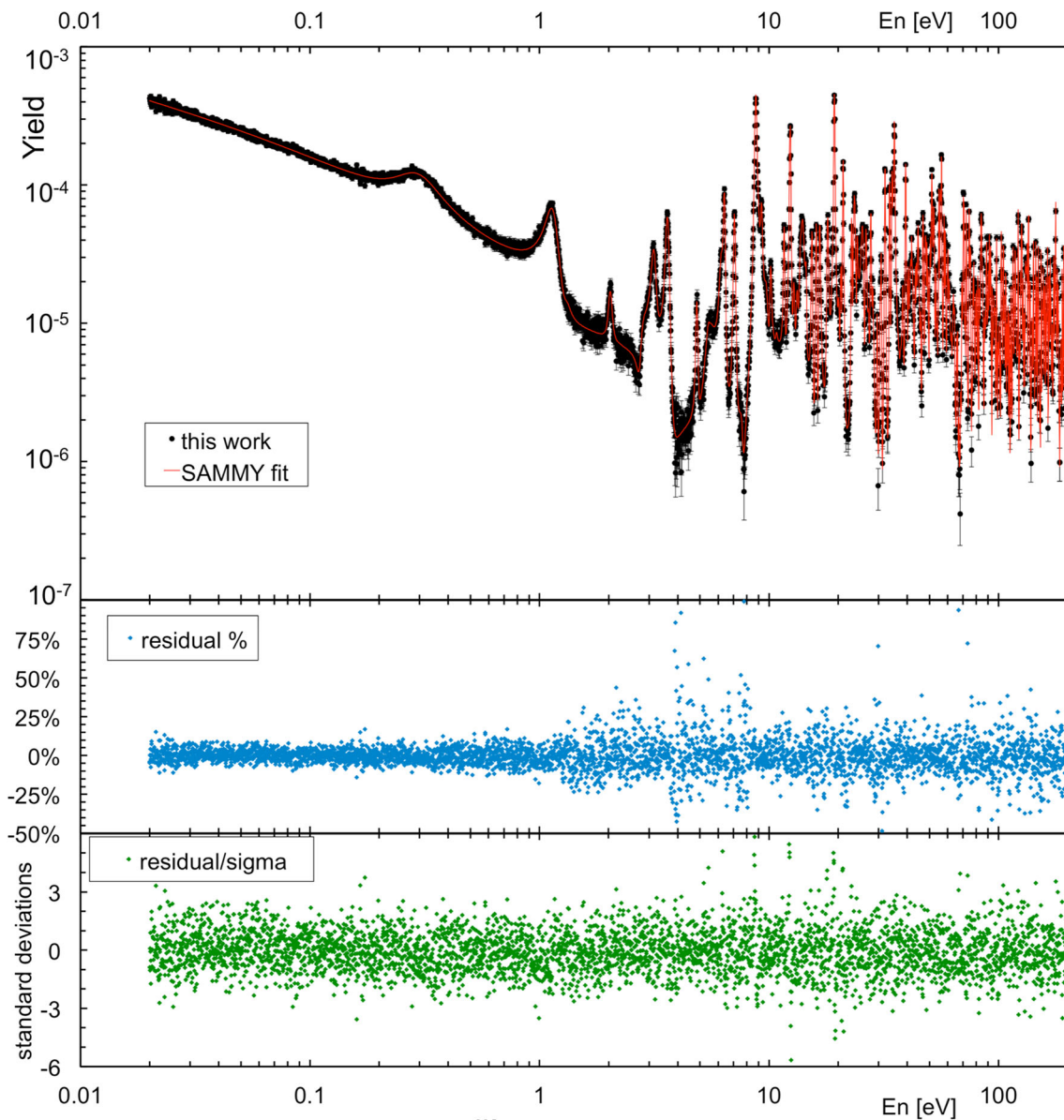


**Fig. 2** Measured yields of the  $^{235}\text{U}(n,f)$  reaction, together with the result of resonance analysis performed with the SAMMY code, using initial parameters from ENDF/B-VIII.0, between 18 meV and 200 eV (top

panel). The residuals between fit and data in percent (middle panel) and in standard deviation units (bottom panel) are also reported in the figure

widths, which may be different in the two major libraries. As a consequence, it is more appropriate, when comparing the experimental data with both libraries, to consider the fission kernel defined as follows,

$$K_f = g \frac{\Gamma_n(\Gamma_{f1} + \Gamma_{f2})}{\Gamma_n + \Gamma_\gamma + \Gamma_{f1} + \Gamma_{f2}} \quad (1)$$

Here  $g$  is the spin factor,  $\Gamma_n$  and  $\Gamma_\gamma$  are the neutron and capture width, respectively, while  $\Gamma_{f1}$  and  $\Gamma_{f2}$  the two fission widths. Figure 4 shows the ratio of the experimental fission kernels to the ones extracted using the ENDF/B-VIII.0 and JEFF-3.3 resonance parameters. The error bars represent the

uncertainty in the SAMMY fit, and are essentially related to the statistical uncertainty on the  $n_{\text{TOF}}$  fission yield data. A very good agreement is observed on average between the present data and both major libraries. Indeed, a weighted average of 1.0037(3) and 1.0016(2) is found for the ratio relative to ENDF/B-VIII.0 and JEFF-3.3, respectively. However, as already mentioned, differences of several percent can be observed for some resonances (or cluster of resonances), mostly small ones, as can be inferred from the large error bars. As for the large discrepancy at 1.3 eV, it casts some doubts on the existence of a resonance in that region, on the tail of the much larger resonance at 1.14 eV. Nevertheless,

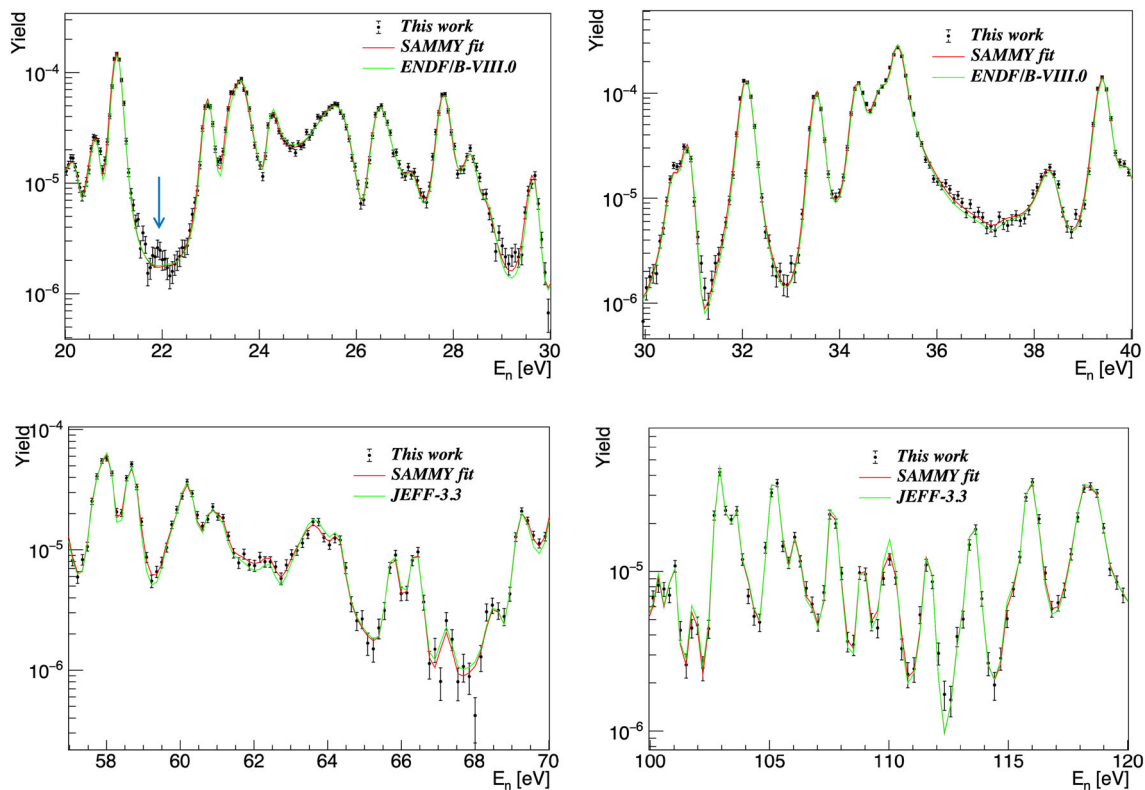


**Fig. 3** Example of SAMMY fits of  $^{235}\text{U}(n,f)$  resonances from the present n\_TOF yield data (red curves and symbols, respectively) compared with yields calculated in SAMMY from resonance parameters of the two most recent libraries, ENDF/B-VIII.0 and JEFF-3.3 (green

curves). Where differences exist, the red and green curve depart from each other. The arrow around 22 eV in the top left plot indicates one of the structures mentioned in the text that was possible to observe in a valley due to the low background

the weighted root mean square of the ratio, that provides an indication of the width of the ratio distribution, turns out to be also small, being less than 1% for both libraries (0.0096 and 0.0064 for ENDF/B-VIII.0 and JEFF-3.3, respectively). This further implies that the two libraries are essentially equivalent and on average closely reproduce the observed n\_TOF resonances up to 200 eV.

### 5 Energy-averaged fission cross sections from thermal to 10 keV neutron energy

While the resonance analysis shown above can provide some indications on the accuracy of the evaluations up to 200 eV, a more complete comparison can be performed, all the way from thermal to 10 keV neutron energy, by considering the average cross sections in wider energy bins. Similar comparisons in this sense have been reported in the literature both between data and libraries (see for example Ref. [6]) and between evaluated data files [7, 11]. In particular, in Refs. [6, 7], it was shown that the cross sections in ENDF/B-VII were higher than the IAEA reference file and Paradela’s data, by

several percent. Following the CIELO project, a modification was introduced in ENDF/B-VIII.0, which adopted the resulting evaluations (mostly based for this reaction on the IAEA reference file). Similarly, the new version of JEFF-3.3 was shown to reproduce the latest standard evaluations [1], as well as the previous one [18] in the neutron energy range 100–2000 eV (see Table 3 in [11]).

Taking advantage of the wide energy range of the present n\_TOF data, we have performed a complete comparison with the two current evaluations, as well as with the previous ENDF/B-VII, with the aim of verifying improvements and/or residual differences. The comparison over the full energy range measured at n\_TOF is shown in Fig. 5, where the reported R values represent the relative difference (i.e. residuals) between the current data and the evaluations.

$$R = 100\% \cdot \left( \frac{\text{data}}{\text{reference}} - 1 \right) \tag{2}$$

For a more detailed analysis the whole neutron energy region from thermal to 10 keV has been divided in different panels in Fig. 6. It has to be considered, however, that between 10 and 30 keV the new evaluations still show an

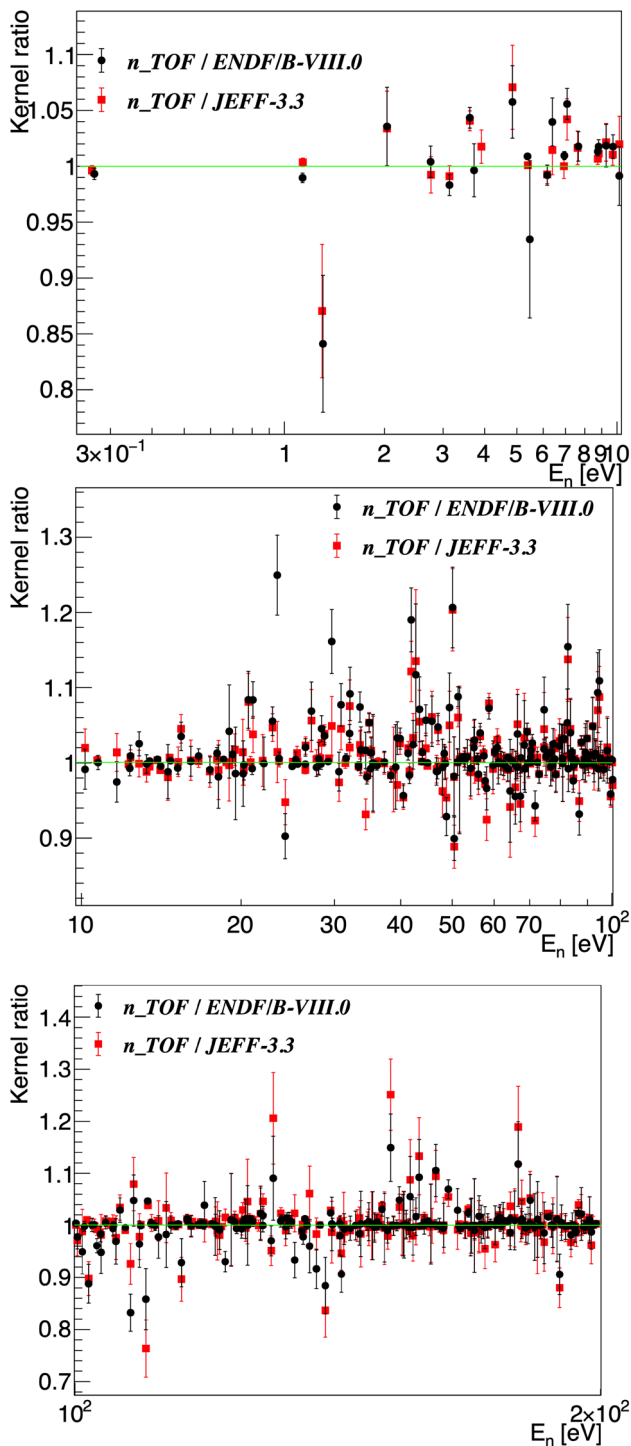


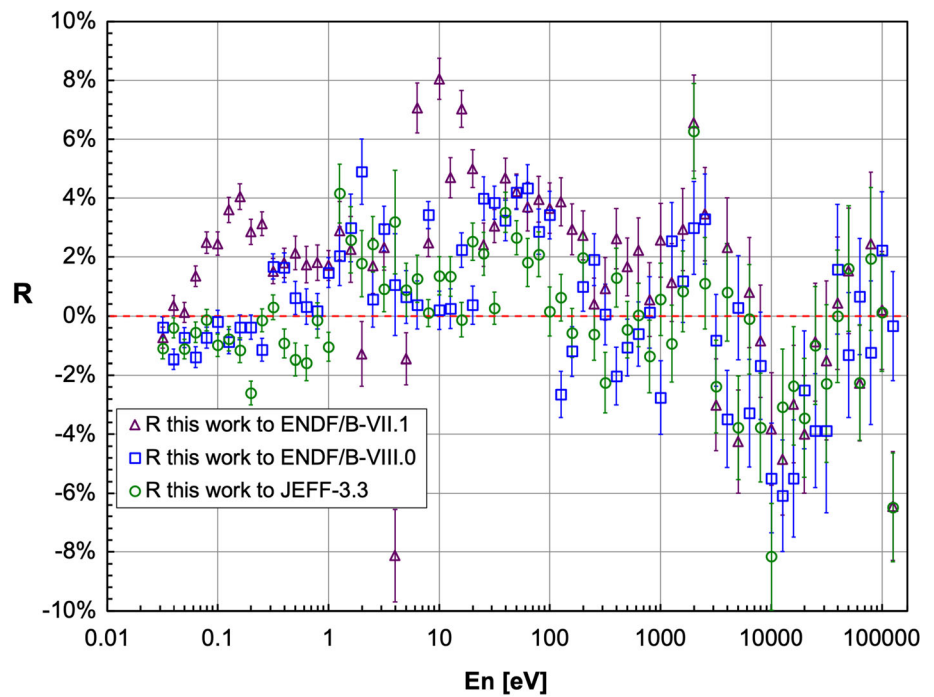
**Fig. 4** Ratio of the  $n_{\text{TOF}}$  fission kernels (determined from SAMMY fit of the resonances), and those calculated from the resonance parameters of the two most recent evaluated data libraries (ENDF/B-VIII.0 and JEFF-3.3). See text for details

important discrepancy relative to the  $n_{\text{TOF}}$  data, as already discussed in Ref. [14], linked to the node description used in the standard evaluation. The chosen energy binning is 10 bins/decade, a value that fulfils the best compromise between the need of a reasonable resolution and that of minimizing statistical fluctuations, in particular in the keV energy region.

The measured energy-averaged cross section was obtained from the fission yield dividing by the areal density of the sample (number of atoms/barn). In this respect, the self-absorption correction is not taken into account, as the small thickness of the  $^{235}\text{U}$  samples used in the  $n_{\text{TOF}}$  measurement results in a negligible effect, of the order of  $10^{-4}$ . For the evaluations, the energy-averaged cross section was derived from the pointwise values, by first interpolating them (according to the library prescriptions) at a very fine resolution (2000 bins/decade), and then integrating the resulting cross section over the same energy intervals of the experimental data (i.e. 10 bins/decade). In the plots, a generally good agreement of the new libraries with the  $n_{\text{TOF}}$  data can be observed, in the whole energy region from thermal to 10 keV. On the contrary, the older ENDF/B-VII library shows a rather large systematic discrepancy, being the  $n_{\text{TOF}}$  data considerably higher than the evaluations by several percent, from a few hundred meV to a few keV. While the underestimate of the cross section in ENDF/B-VII in the recently established standard from 7.8 to 11.0 eV had been previously reported, as compared to the IAEA reference value (see for example Ref. [6]), a somewhat unexpected finding is the discrepancy in the 100–300 meV neutron energy. In these two energy ranges, the recent re-evaluation within the CIELO project, adopted in the most recent libraries, has led to a substantial improvement of the cross section, relative to previous evaluated data, as demonstrated by the very good agreement with the present  $n_{\text{TOF}}$  data. However, some discrepancies can still be noted even for the new libraries. At low energy, up to approximately 1 eV, the  $n_{\text{TOF}}$  cross sections are slightly lower than JEFF-3.3 evaluations, by around 1%, while they are in good agreement with the ENDF/B-VIII.0 evaluations. On the contrary, the two libraries mostly agree in the range 1–100 eV, but the  $n_{\text{TOF}}$  data are systematically higher than both of them at a few eV and between 20 and 80 eV. It is interesting to note that in that range there were only slight changes in the new evaluations with respect to the previous ones (see comparison with ENDF/B-VII). It should be also noted that, as shown previously, important differences are observed in the resonances in that range, therefore calling for a better evaluation of the resonance parameters in future library releases.

In the 100 eV to 1 keV range, no particular problems are observed, except for a 2% discrepancy around 200 eV neutron energy. Finally, the comparison in the 1 to 10 keV range highlights a problem around 2 keV. This energy corresponds approximately to the limit of the Resolved Resonance

**Fig. 5** Relative difference  $R$  between the  $^{235}\text{U}(n,f)$  energy-averaged cross section measured at n\_TOF in the full neutron energy range, from thermal to 170 keV, and the evaluated cross section from major current data libraries, namely ENDF/B-VIII.0 and JEFF-3.3. The discrepancy with the older ENDF/B-VII.1 library is also shown for comparison. The average was calculated over 10 bins/decade



Region in the libraries, and at least part of the observed discrepancy could be attributed to the difference of treatment in the evaluation between the RRR and URR. After a careful investigation, however, we have come to the conclusion that most probably this is not the reason for the differences between the present n\_TOF data and evaluations. A comparison with previous data, in particular Paradela's ones [6], shows a large difference between 2 and 3 keV (a difference is also observed, relative to Weston [19], although smaller). In this region, the n\_TOF flux exhibits a small dip, as it can be appreciated in the neutron flux determined in the measurement here reported from the  $^6\text{Li}(n,t)$  and  $^{10}\text{B}(n,\alpha)$  reactions (see Fig. 11 of Ref. [14]). The dip can be attributed to the 2.63 keV resonance in the total cross section of  $^{64}\text{Zn}$  (dominated by elastic scattering). Zinc is present in the neutron source at n\_TOF, being a 0.2% contaminant of the Al alloy 6082, used for the window at the interface between the spallation target and the vacuum beam line. Being the dip small and barely visible in the adopted energy distribution of the neutron beam in EAR1 [13], it was not accounted for in the analysis of Ref. [6], in which the cross section was extracted relative to that energy distribution. It can therefore be concluded that the difference relative to the IAEA reference file observed in Ref. [6] around 2 keV neutron energy is essentially related to the mentioned absorption dip, and it cannot be excluded that a similar problem might also be present in other previous datasets, as already mentioned. As it can be noted in Fig. 6, in the recent evaluations the cross section has been increased in that energy bin, and agree better with the present data. A reminiscence of the problem might however

still be present at slightly lower energy, being the n\_TOF data in the bin at 2 keV higher, by 3% and 6% relative to ENDF/B-VIII.0 and JEFF-3.3, respectively. A re-evaluation of the cross section in this energy region might therefore be needed to account for the new evidences here discussed.

The overall performance of the two most recent evaluated data libraries, in reproducing the new n\_TOF data reported here can be inferred from Fig. 7, that shows the weighted average deviation of the evaluated cross sections from the present data, in the full energy range examined, i.e. between thermal and 10 keV, and in four sub-ranges. The employed weight is the inverse of the square of the statistical error. From the figure, one can appreciate the large improvements in the most recent libraries, following the CIELO project, relative to the previous one. Overall, both ENDF/B-VIII.0 and JEFF-3.3 agree with the new data within less than half a percent, a remarkable result, in particular if compared with the systematic difference of the present data relative to ENDF/B-VII by 2%. However, it should be noted that such a good overall agreement with the most recent evaluations is the result of positive and negative deviations in different energy regions that compensate each other. Nevertheless, in all ranges the agreement with the two current evaluated data libraries is around 1%, except for the 1–100 eV range, where a 2% difference is observed for ENDF/B-VIII.0, mostly related to a problem in the 20–80 eV region, as shown in Fig. 4 by the ratio between the resonance kernels and in Fig. 6 by the comparison of the energy-averaged cross sections.

It is also interesting to compare the present data with a few previous experimental datasets, that have been considered in

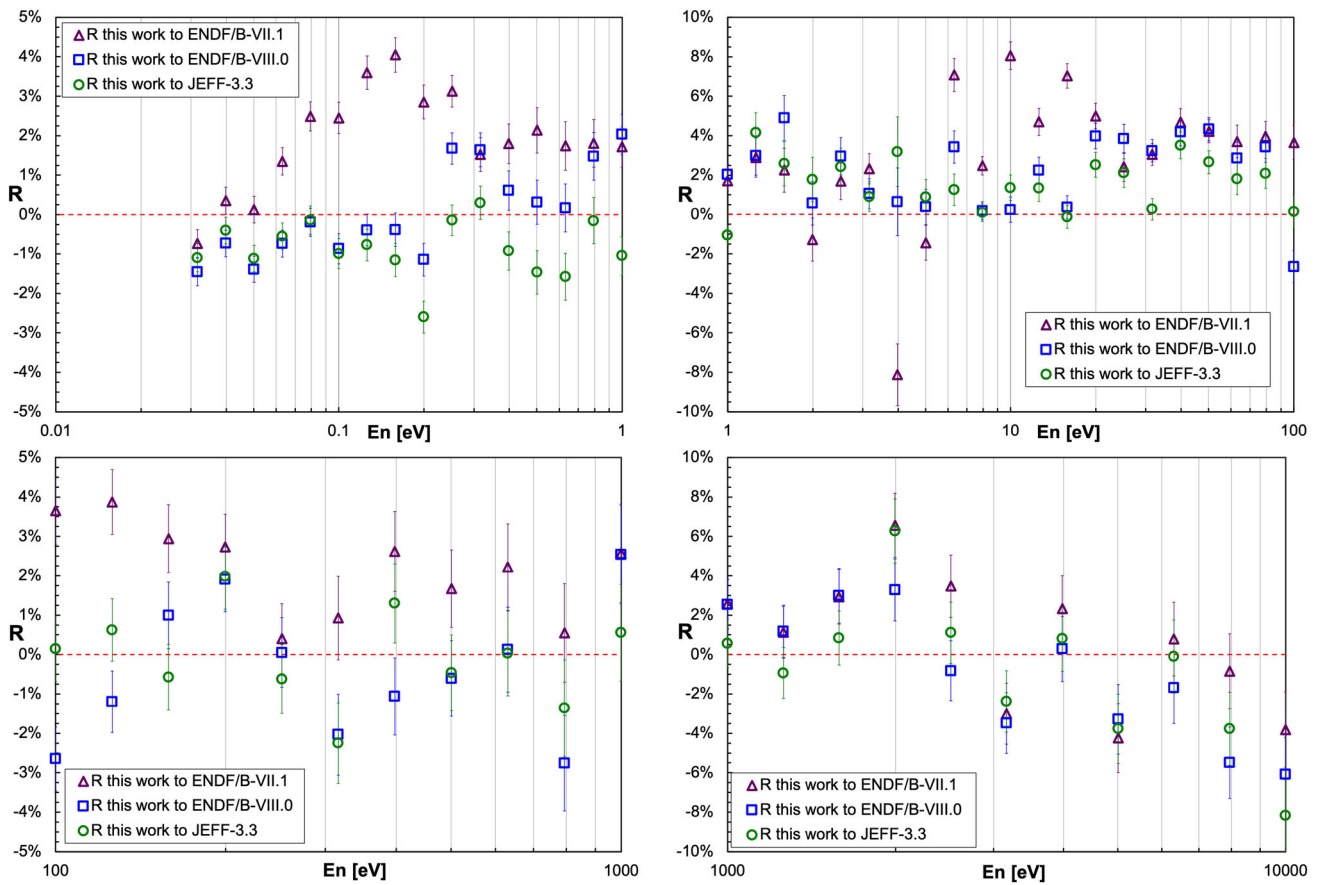


**Fig. 6** Comparison of the present n\_TOF cross section averaged in 10 bins/decade, with energy-averaged cross sections from the two most recent evaluated data libraries, ENDF/B-VIII.0 and JEFF-3.3. The older ENDF/B-VII library is also included in the comparison, showing the substantial improvement in current evaluations relative to previous ones. In some energy regions, differences of several percent are still present

in current evaluated files. The four panels represent different neutron energy ranges, from thermal to 1 eV (upper left panel), from 1 to 100 eV (upper right), from 100 eV to 1 keV (bottom left) and finally from 1 to 10 keV (bottom right). The purple triangles show the ratio between the present data and ENDF/B-VII, the blue squares the ratio to ENDF/B-VIII.0 and the green circles the one to JEFF-3.3

**Fig. 7** Weighted average of the relative difference R between the n\_TOF data of this work and the most recent evaluations, as well as a previous version of the ENDF library, in the overall energy range from thermal to 10 keV, and in smaller ranges. The error bars represent the statistical uncertainty of data. The systematic uncertainty, not included, is due to the normalization to the 7.8–11 eV integral and is 1.3% [14]

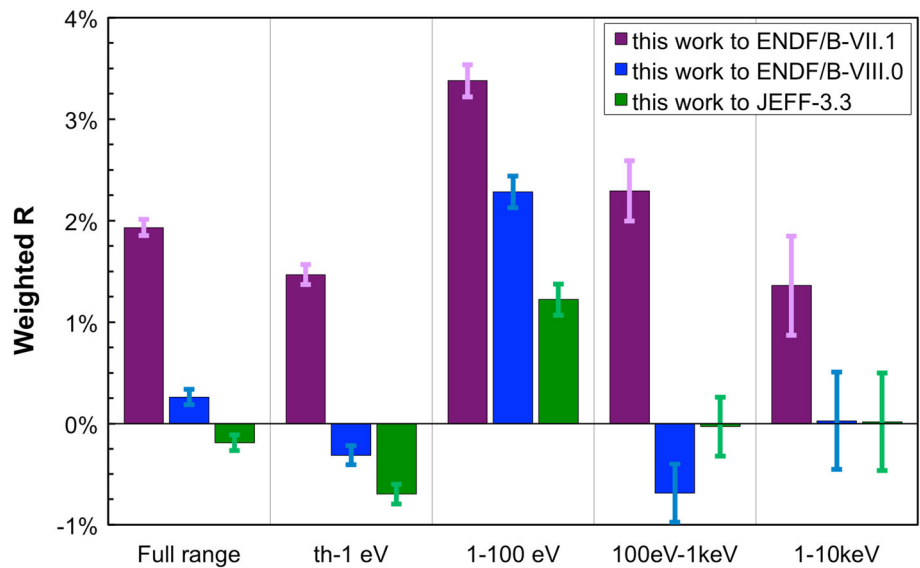


**Fig. 8** The relative difference  $R$  between the present dataset and a selection of previous experimental results: previous n\_TOF data of Paradela et al. [6], Weston [19], Mostovaya [20] and Blons [21]

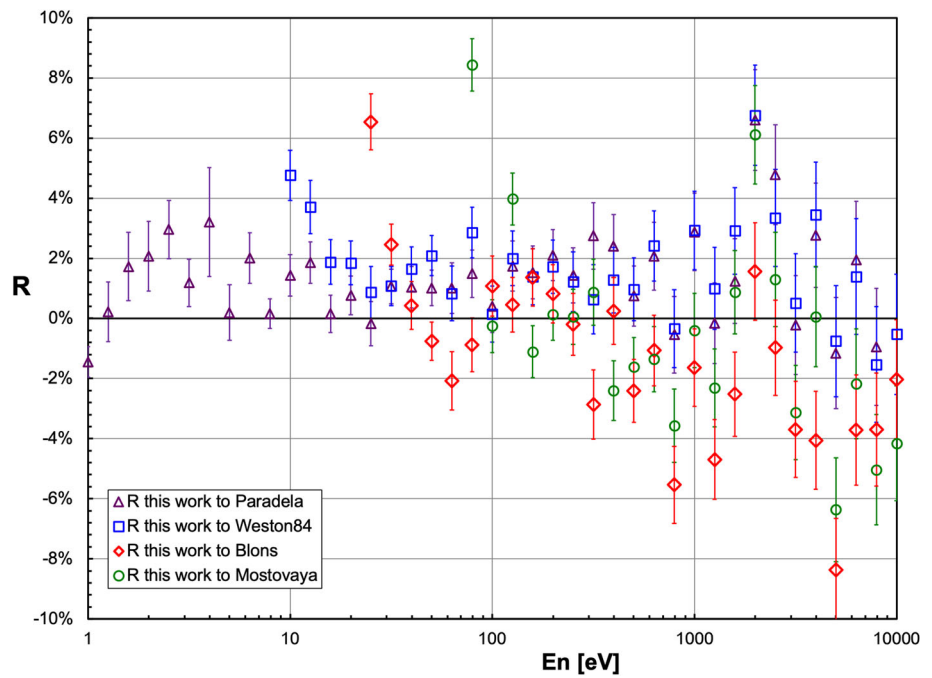
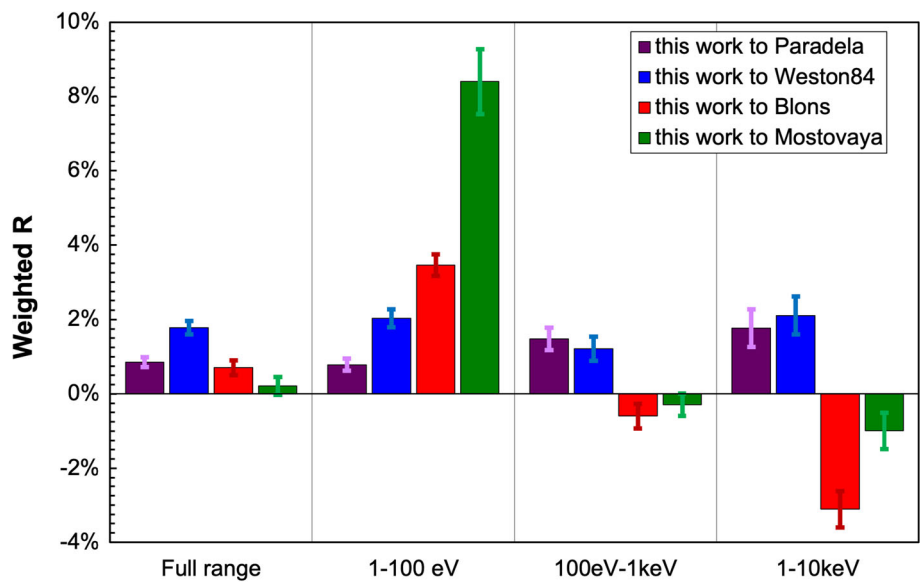


**Fig. 9** Weighted average of the relative difference  $R$  between the present dataset and a selection of previous experimental results: previous n\_TOF PPAC data of Paradela [6], Weston [19], Mostovaya [20] and Blons [21]. The error bars represent only the combination of the statistical uncertainty of data. In the range from thermal to 1 eV neutron energy it is not possible to perform a comparison, because of the lack of data in that region for earlier measurements



past and current evaluations. In particular, the comparison has been done relative to Paradela’s data [6], and the earlier measurements of Weston [19], Mostovaya [20], Blons [21]. Such a comparison is shown in Fig. 8. Figure 9 shows the weighted average of the relative difference  $R$  for the n\_TOF data of this work with respect to previous results in selected energy ranges. It should be considered that the range covered by the present and earlier datasets do not completely overlap, being 0.66 eV to 10 keV for Paradela [6], 9.73 eV to 200 keV for Weston [19], 78 eV to 20 keV for Mostovaya [20], and 17.5 eV to 30 keV for Blons [21]. In each case the

comparison was performed only in the region where the previous data overlap, totally or partially, with the present ones. All previous datasets considered in this work have no data from thermal to 1 eV energy, so that no comparison could be performed in that region. Relative to the data of Weston [19], the results presented here are systematically higher by 1 to 2%, while they are higher relative to Paradela’s data [6] by 0.7% in the 1–100 eV range and 1.8% in the 1–10 keV region. This difference is most probably related on the one hand to a slightly less accurate normalization of those data, and on the other hand to the larger uncertainty in the neutron

**Table 1** Energy-averaged cross section from 100 eV to 2 keV, calculated from the IAEA standards of 2009 [18] and 2017 [1], the latest JEFF-3.3 evaluations (all from Table 3 of Ref. [11]), and the n\_TOF data reported in this work. The integrated cross section in the 7.8–11.0 eV range, used in this work for normalization, is also included in the Table. Its quoted uncertainty is statistical only

	IAEA 2009	IAEA 2017	JEFF-3.3	This work
(eV)	(b eV)	(b eV)	(b eV)	(b eV)
7.8–11	246.4(12)	247.5(30)	246.9	247.5 (11)
(eV)	(b)	(b)	(b)	(b)
100–200	21.17(11)	21.3(3)	21.02	21.07(10)
200–300	20.69(11)	20.8(3)	20.77	20.99(14)
300–400	13.13(7)	13.2(2)	13.22	13.04(13)
400–500	13.78(8)	13.9(2)	13.49	13.66(14)
500–600	15.17(9)	15.2(2)	15.2	15.16(17)
600–700	11.51(7)	11.57(15)	11.53	11.55(15)
700–800	11.10(6)	11.15(14)	11.1	11.19(16)
800–900	8.21(5)	8.25(11)	8.15	8.01(14)
900–1000	7.50(4)	7.54(10)	7.37	7.42(14)
1000–2000	7.30(4)	7.34(10)	7.29	7.36(06)

**Table 2** The cross section in barns interpolated at neutron energy  $E_n = 25.3$  meV from the data of this work, as compared with the reference values in the libraries and the IAEA standard value of 2017. The quoted uncertainty is statistical only

IAEA 2017	ENDF/B-VII	ENDF/B-VIII.0	JEFF-3.3	This work
(b)	(b)	(b)	(b)	(b)
587.3	585.0	586.7	584.5	586.2 (33)

flux used as reference for extracting the cross section, in particular above 1 keV. These elements gave rise to a systematic uncertainty of 2.6% whereas the uncertainty in our current data is 1.3%. Finally, an almost perfect overall agreement, within 1%, can be observed between present data and the ones from Mostovaya [20] and Blons [21], although in both cases this is the result of a combination of a positive difference from 1 to 100 eV, and a negative one at higher energy (of a few per mill from 100 eV to 1 keV and around 1% and 3% in 1–10 keV range, for Mostovaya and Blons, respectively).

The n\_TOF energy-averaged cross sections from 100 eV to 2 keV in several energy groups are compared with the IAEA reference files and with the JEFF-3.3 evaluations in Table 1 (that essentially reproduces Table 3 of Ref. [11] with the addition of the present results). The table also includes the energy-integrated cross section between 7.8 and 11 eV, now adopted as an additional standard. It is interesting to note the almost perfect agreement between the present data and the IAEA reference files of 2009 and 2017, that have now been adopted in the latest version of the ENDF/B library, as well as with the new JEFF-3.3 evaluation, demonstrating the reliability on average of this last library as well as of the IAEA reference file. In Table 2 we report the interpolated cross section value at 25.3 meV along with the reference values in the libraries and the IAEA standard value. As previously mentioned, the agreement within a few per mill between the

present data and the standard value (and that of major evaluations) provides high confidence on the accuracy of the present dataset.

## 6 Conclusions

The  $^{235}\text{U}(n,f)$  cross section was determined with high accuracy and high resolution from thermal to 170 keV, in a dedicated measurement performed at n\_TOF in the experimental area at the end of the 184 m long flight-path. The cross section was extracted from a direct ratio measurement, relative to the  $^6\text{Li}(n,t)$  and the  $^{10}\text{B}(n,\alpha)$  standard reactions. A compact, Si-based setup placed in the neutron beam was used for the detection of the reaction products. Data have been collected both in the forward and in the backward direction, to minimize the uncertainty related to angular anisotropy in the charged particle emission from the reference reactions. The normalization has been performed in the 7.8–11.0 eV energy region, using the recommended IAEA standard value of 247.5 (30) b-eV. The resulting cross sections were checked against the standard at thermal and 150 keV neutron energy. This procedure has resulted in a very low uncertainty of 1.3%. Such a high accuracy, combined with the high resolution and the wide energy range covered, makes the data reported here among the most complete and reliable ever collected in the RRR and URR.

The results have been compared with recent evaluated data libraries, that have included the outcome of the CIELO project, devoted to improving cross section evaluations for applications. In particular, we have compared resonance fission kernels and energy-averaged cross sections with the values extracted from the two most recent evaluated libraries, ENDF/B-VIII.0 and JEFF-3.3, as well as with the previous ENDF/B-VII library. An overall good agreement is observed, within 0.5%, with the new evaluations, with a significant improvement relative to previous versions. However, a more detailed comparison shows that discrepancies still exist between present data and all evaluations in some specific energy regions, namely at a few eV, between 20 and 80 eV, and around 2 keV. The availability of the present data on EXFOR might help to improve future evaluations in these regions, and to solve remaining discrepancies.

**Funding** Open access funding provided by CERN (European Organization for Nuclear Research).

**Data availability statement** This manuscript has associated data in a data repository [Authors' comment: All the data presented in this manuscript are available on Experimental Nuclear Reaction Data (EXFOR).]

**Open Access** This article is licensed under a Creative Commons Attribution 4.0 International License, which permits use, sharing, adaptation, distribution and reproduction in any medium or format, as long as you give appropriate credit to the original author(s) and the source, provide a link to the Creative Commons licence, and indicate if changes were made. The images or other third party material in this article are included in the article's Creative Commons licence, unless indicated otherwise in a credit line to the material. If material is not included in the article's Creative Commons licence and your intended use is not permitted by statutory regulation or exceeds the permitted use, you will need to obtain permission directly from the copyright holder. To view a copy of this licence, visit <http://creativecommons.org/licenses/by/4.0/>.

## References

1. A.D. Carlson et al., Nucl. Data Sheets **148**, 143 (2018)
2. M.B. Chadwick et al., Nucl. Data Sheets **148**, 189 (2018)
3. [Online]. <https://www-nds.iaea.org/INDEN/>.
4. C. Guerrero et al., Eur. Phys. J. A **49**, 27 (2013)
5. N. Colonna et al., Eur. Phys. J. A **56**, 48 (2020)
6. C. Paradela et al., EPJ Web Conf. **111**, 02003 (2016)
7. R. Capote et al., Nucl. Data Sheets **148**, 254 (2018)
8. D.A. Brown et al., Nucl. Data Sheets **148**, 1 (2018)
9. [Online]. Available: <https://www.nndc.bnl.gov/ndf-b8.0/>.
10. I. Duran et al., EPJ Web of Conferences **211**, 02003 (2019)
11. A. Plompen et al., Eur. Phys. J. A **56**, 181 (2020)
12. [Online]. <https://www.oecd-nea.org/dbdata/jeff/jeff33/>.
13. M. Barbagallo et al., Eur. Phys. J. A **49**, 156 (2013)
14. S. Amaducci et al., Eur. Phys. J. A **55**, 120 (2019)
15. V.V. Zerkin et al., Nucl. Instr. Meth. A **888**, 31 (2018)
16. [Online]. <https://www-nds.iaea.org/standards/>.
17. N. M. Larson, Report ORNL/TM-9179/R8, (2008).
18. A.D. Carlson et al., Nucl. Data Sheets **110**, 3215 (2009)
19. L.W. Weston, J.T. Todd, Nucl. Sci. Eng. **88**, 567 (1984)
20. T.A. Mostovaya et al., Proceedings of the 5th All Union Conference on Neutron Physics, vol. 3, pp. 30–32, (1980).
21. J. Blons et al., Nucl. Sci. Eng. **51**, 130 (1973)